ELSEVIER

Thermochimica Acta 266 (1995) 97–111

thermochimica acta

# Modulated differential scanning calorimetry in the glass transition region ☆

Andreas Boller [a,b,*], Christoph Schick [c], Bernhard Wunderlich [a,b]

[a] *Department of Chemistry, The University of Tennessee, Knoxville, TN 37996-1600, USA*
[b] *Chemistry and Analytical Sciences Division, Oak Ridge National Laboratory, Oak Ridge, TN 37831-6197, USA*
[c] *Universität Rostock, Fachbereich Physik, Universitätsplatz 3, D-18051 Rostock, Federal Republic of Germany*

**Abstract**

Modulated differential scanning calorimetry (MDSC) presents two time scales to the measurement of the glass transition, a fast one, fixed by the modulation time period, and a slow one, fixed by the average, underlying heating or cooling rate. The same situation arises in dynamic mechanical and dielectric measurements. The various time effects on the glass transition are discussed and documented with experiments on the reference material polystyrene. It will be shown that MDSC can measure the glass transition temperature largely independent of the thermal history (and the heating or cooling rates), but dependent on the modulation frequency. This distinguishes MDSC from standard calorimetry that can measure accurate data on the glass transition only on cooling, a mode of operation often neither convenient nor very precise.

*Keywords:* Ageing; Dynamic mechanical analysis; Glass transition; Hysteresis; MDSC; Modulated calorimetry; Polystyrene; Quasi-isothermal measurement

## 1. Introduction

Modulated differential scanning calorimetry (MDSC) is a recent variation of differential scanning calorimetry with constant heating or cooling rates (DSC) [1–4]. The MDSC used in this research is modulated at the block temperature $T_b(t)$ with a sinusoidally changing amplitude that is governed, as in standard DSC, by the

* Corresponding author.

☆ Dedicated to Professor Hiroshi Suga on the Occassion of his 65th birthday. Presented in part at the 23rd Conference of the North American Thermal Analysis Society, Toronto, Canada, September 25–28, 1994.


*SSDI* 0040-6031(95)02552-9

temperature measured at the sample position:

$$T_b(t) = T_0 + qt + A_{T_b} \sin \omega t \tag{1}$$

where $q$ is the underlying, constant heating rate and $T_0$, the initial isotherm at the beginning of the scanning experiment. The modulation frequency $\omega$ is equal to $2\pi/p$ in units of rad/s, with $p$ representing the duration of one cycle [s]. Measurements can then be made as soon as steady state is reached, either under close-to-isothermal conditions ($q = 0$) [5], or by adding a linear temperature ramp $qt$. The sample and reference temperatures, $T_s$ and $T_r$, respectively, are given at steady state by:

$$T_s = T_0 + qt - \frac{qC_s}{K} + A_{T_s} \sin(\omega t - \varepsilon) \tag{2}$$

$$T_r = T_0 + qt - \frac{qC_r}{K} + A_{T_r} \sin(\omega t - \phi) \tag{3}$$

where $K$ is the Newton's Law constant (assumed to be the same for sample and reference, dimension $J\,s^{-1}\,K^{-1}$) and $C_s$ and $C_r$ represent the heat capacities of the sample and reference calorimeters. The calorimeters usually consist of close-to-identical aluminum pans with and without sample, giving heat capacities $C' + mc_p$ or $C'$, respectively (where $C'$ = pan heat capacity, $m$ = sample mass, and $c_p$ = specific heat capacity of the sample). The maximum heating and cooling rates caused by the modulation are given by $A_{T_s}\omega$ [see Eq. (2), $dT_s/dt$ at phase angles $(\omega t - \varepsilon) = 0$ and 180°.]. A detailed mathematical description of MDSC of this type has been given recently [6]. In MDSC one has, thus two time scales to consider, the underlying heating rate and the period of modulation. Calorimetry of any material that undergoes time-dependent processes needs thus special attention [7, 8].

The glass transition is the major time-dependent transition in condensed matter [7] It separates corresponding solid and mobile states of a given amount of disorder. In solids, small-amplitude vibrations are the dominant thermal motion. In the mobile states, additional large amplitude motion, such as translation, rotation, and internal rotation (Conformational mobility) cause the typical macroscopic mobility. Fig. 1 shows a schematic of the basic condensed phases [9]. Between the melt (liquid) and the crystal three mesophases are located. The liquid crystal is distinguished from the liquid by some orientational order (and reduced rotational motion) due to the presence of rod-like or disc-like mesogens [10]. The plastic crystal shows long-range crystalline order, but orientational motion (rotation) is possible within the crystal, due to a close-to-spherical shape of the molecules that show a plastic crystalline phase [11]. Conformationally disordered crystals (condis crystals) have some or complete conformational disorder and mobility, but long-range orientational and positional order [12]. The crystals, melt, and the mesophases are linked by first-order transitions during which they change their order, as indicated on the right side of the figure. Also shown are typical entropies connected with the various types of order.

Besides the crystalline state, there are four glassy solids indicated. Each glass is linked to the corresponding mobile phase through a glass transition, as shown on the left side of the figure. Each fully mobile part of the molecule (bead) contributes the indicated change to the heat capacity at the glass transition. The basic glass transition is known

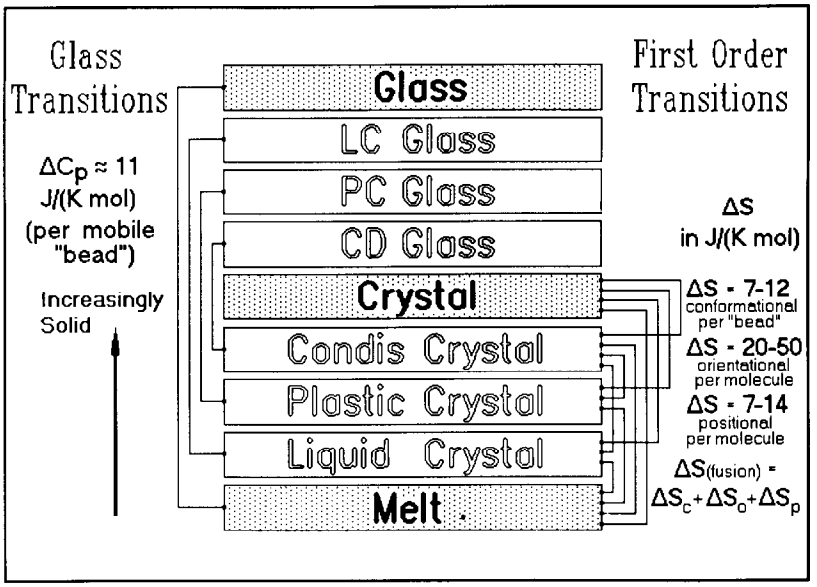


Fig. 1. Schematic of the transition regions for the classical condensed phases (dotted areas and full lettering) and the mesophases. Glass transitions and observed first-order transitions are indicated by the connecting lines. The empirically observed (approximate) entropies and heat capacities are listed. Drawn after [9].

for many years [13]. It is seen on vitrification of a liquid that is unable to crystallize for kinetic or structural reasons. The detailed definitions of the glass transition were recently reviewed in a symposium of the American Society for Testing of Materials (ASTM) [14]. As is indicated in Fig. 1, mesophases may also show glass transitions since they carry out some large-amplitude motion. These and other glass transitions of partially ordered materials were also reviewed recently [15]. The first observation of glasses of liquid crystals is credited to Vorlaender [16]. Considerable progress in the understanding of glass transitions of the mesophase crystals was achieved by Suga and Seki who calorimetrically analyzed the glass transitions in several liquid crystals with rod-like mesogens, such as cholesteryl hydrogen phthalate [17] and N-(*o*-hydroxy-*p*-methoxybenzylidine)-*p*-butylaniline [18] and disc-like benzene hexa-*n*-alkanoate mesogens [19], as well as plastic crystals, such as cyclohexanol, cyclohexene, and 2,3-dimethyl butane [20]. The glass transitions in condis crystals were reviewed in Ref. [12].

In this paper the time and frequency dependence of the glass transition of polystyrene will be analyzed using MDSC. Atactic polystyrene is chosen as a typical glass former. Similar results are expected for most other glasses, even mesophases [9].

## 2. Experimental details

### 2.1. Instrumentation, calibration, and measurements

A commercial Thermal Analyst 2910 system from TA Instruments Inc. with modulated DSC (MDSC) was used for all measurements. Dry $N_2$ gas with a flow rate of

10 ml/min was purged through the sample. Cold nitrogen, generated from liquid nitrogen was used for cooling. Sample masses were about 9 mg, and for calibration 24.9 mg of sapphire was used. The pan weights were always about 23 mg and matched on sample and reference sides.

Heat capacities were calibrated with a sapphire standard [21] as a function of modulation frequency and at each chosen temperature, as described earlier [5]. It was made sure that the modulation amplitude of the sample temperature, $A_{T_s}$, was chosen so that steady state could approximately be maintained within the rather wide changes in heating rates produced during the modulation. For detailed graphs of the limits of modulation as a function of temperature and cooling capacity see Ref. [5]. The temperature calibration was carried out using the onsets of the transition peaks for cyclohexane (186.1 and 279.7 K), naphthalene (353.42 K), indium (429.75 K) and tin (505.05 K).

Three kinds of experiments have been carried out. 1) To see the effect of modulation frequency, quasi-isothermal measurements of the heat capacity of polystyrene were made in sequence at 24 temperatures covering the glass transition region starting at about 400 K and finishing at about 340 K. The same maximum heating and cooling rates of 3.8 K/min were set in the modulation by using the modulation amplitudes $A_T = 0.3$, 0.6, and 1.0 K, coupled with periods $p$ of 30, 60, and 99 s, respectively (frequencies $\omega = 0.21 - 0.06$ rad/s). 2) A continuous, nonisothermal series of thermal analyses was done at $q = 1$ K/min heating and cooling rates in the same temperature range, but with varying maximum heating and cooling rates in the modulation. At a modulation period $p$ of 80 s the amplitudes were chosen to be $A_T = 0.25$, 1.0, and 10 K (maximum heating rates 1.18 – 47.1 K/min). The measurements were supported by adding quasi-isothermal experiments at 378, 373, 370.5, 367.5, 365.5, 363, and 358 K, with variable maximum heating and cooling rates in the modulation. 3) The approach to equilibrium was tested by cooling the sample in different experiments at 10 K/min for thermal analysis ($p = 80$ s and $A_T = 1.0$ K).

### 2.2. Data treatment

The recording and deconvolution of the signals described by Eqs. (2) and (3) is done by the software of the chosen MDSC. Details are given, for example, in Refs. [5] and [6]. The reversible (reversing) heat capacity is extracted from the modulation amplitudes and is given, for the case of equal mass of the empty sample and reference pans, by:

$$mc_p = \frac{A_\Delta}{A_{T_s}} \sqrt{\left(\frac{K}{\omega}\right)^2 + C'^2} \tag{4}$$

with $A_\Delta$ representing the modulation amplitude of the temperature difference $T_r - T_s$ (proportional to the heat flow $HF$, phase difference $\delta$).

Fig. 2 shows typical recording from experiments of kind 1). In the upper curves the temperature $T_s$ and the heat flow $HF$ are represented for a series of runs on $Al_2O_3$ at 383.3 K ($q = 0$) at modulation periods of $p = 99$, 30, and 60 s (from left to right). For evaluation the last 10 minutes of each recording, which consisted of 200 points each,

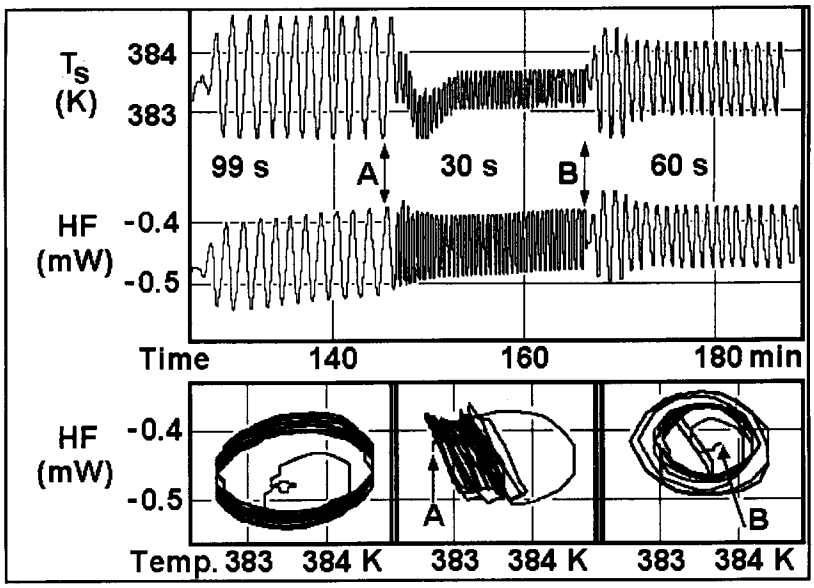


Fig. 2. Sample traces of the quasi-isothermal calibration runs of kind 1) experiments on $Al_2O_3$ at 383.8 K ($q = 0$). Top curves: Modulated sample temperatures of periods $p = 99, 30$, and 60 s (left to right). Bottom row: plots of HF (proportional to $\Delta T$) vs. $T_s$. Points A and B indicate the start of the bottom graphs.

were evaluated. The standard deviations for the final data of these three runs in terms of heat capacity were 0.05, 0.1, and 0.06%, typical for the measurements carried out in this paper. The quality of the measurement can also be judged from plots of *HF* (proportional to $\Delta T$) *vs.* $T_s$, as shown in the bottom row of Fig. 2. The beginnings of the center and right traces, A and B, respectively, are marked in the top and bottom graphs. The approach to steady state and the drift in heat flow (ordinate) is clearly visible in the experiment with a 99 s period. The experiment with the 30 s period shows an initial drift in temperature (abscissa), while the experiment with a 60 s period revealed a longer time period for reaching steady state in the modulation amplitude. All these potential error sources for standard DSC are in this case largely eliminated by measuring only effects with the set modulation frequency and waiting until steady state has been reached.

The heat capacity computed by the MDSC software is equal to:

$$mc_p = K_C \times \frac{\text{smoothed}\langle A_{HF}\rangle}{\text{smoothed}\langle A_{T_s}\rangle} \times \frac{1}{\omega} \tag{5}$$

where $K_C$ must be calibrated at the given temperature and frequency:

$$K_C = C_p(Al_2O_3, \text{literature}) \times \frac{\text{smoothed}\langle A_{T_s}\rangle}{\text{smoothed}\langle A_{HF}\rangle} \times \omega \tag{6}$$

with $A_{T_s}$ and $A_{HF}$ representing the calibration run data as shown in Fig. 2. The literature heat capacity of the calibration substance, sapphire, is given in Ref. [21]. The

advantage of the use of the modulation for measurement lies, thus, in the elimination of any slow drifts of the calorimeter caused inadvertently or by irreversible processes in the sample. It is even possible to measure, for example, heat capacity in the presence of slow oxidation or evaporation without errors beyond the effects of permanent changes in composition and mass [1–4], see also [22]. For the present research, the hysteresis effects at the glass transition shows only in the total and nonreversing heat flows.

The total heat flow $\langle HF(t)\rangle$ is evaluated in MDSC by taking sliding averages over full cycles of modulation. Since the sine functions average to zero over every full cycle, this type of averaging eliminates the modulation effect and gives thus data similar to standard DSC, as shown in Fig. 3. A full treatment of the relationship of the total heat flow to heat capacity is available in Ref. [7], p. 161, Eqs. (9–14). The common analysis is in this case carried out by assuming that at steady state $q$ can be equated to $dT_r/dt$ (i.e. $dt = dT_r/q$) and gives:

$$mc_p = K\Delta T/q + [(K\Delta T/q) + C']d\Delta T/dT_s \tag{7}$$

Only if the actual baseline is close to horizontal, so that $d\Delta T/dT_s \approx 0$, is the heat capacity of the sample easily assessed as $K\Delta T/q$. Under all other circumstances, the recording of $\Delta T$ (or $HF$) misses a certain portion of the heat capacity because sample and reference do not change their temperature at the same rates. Fortunately the error

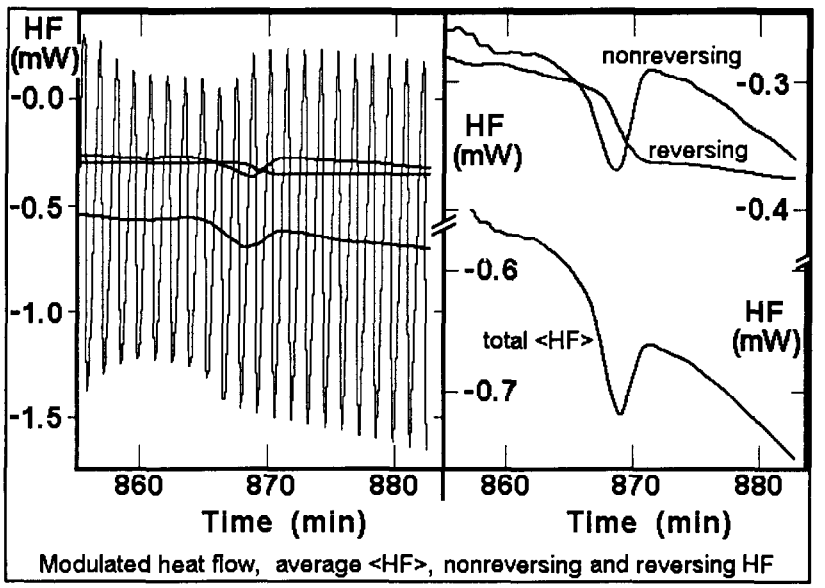


Fig. 3. Separation of reversing and nonreversing contributions to the apparent heat capacity. Left figure: Modulated heat flow HF, sliding averages $\langle$HF$\rangle$ (in the center of HF, averaged over one modulation cycle), and, at lower negative ordinates, the evaluated reversing and nonreversing heat capacities. Right figure: expanded scale drawings of the three sliding averages. Experiment of kind 3), $q = 2$ K/min, $p = 80$ s, $A_{T_s} = 1.0$ K, after annealing for 240 min at 353.15 K.

is usually small (about 1% for 45° slopes if the sensitivity of recording $\Delta T$ is 100 × that of $T$).

The irreversible (nonreversing) part of the heat capacity is then taken as the difference between total and reversible heat capacity. It contains all the effects due to heat loss and different heating rates of sample and reference and is thus less precise. An example of separation of reversible heat capacity and irreversible hysteresis in the present experiments is shown in Fig. 3.

### 2.3. Samples

The sapphire disc and indium for calibration were supplied with the accessory kit of the MDSC instrument. A standard sample of polystyrene of MW = 100000, $M_w/M_n < 1.06$ was bought from Polyscience. Inc., Warrington, PA. The heat capacity of such standard polystyrene is available in the ATHAS data bank [23] and the kinetics of the glass transition has been studied in detail earlier [24]. The glass transition is 373 K for the typical cooling rates of 1–10 K/min. The increase in heat capacity is 30.8 J $K^{-1}$ $mol^{-1}$ of repeating unit (104.2 Da). The change in glass transition temperature with cooling rate was found to be 4.03 log $q$ ($q$ in K/min) [24].

## 3. Results

The data of the measurements of kind 1) are illustrated by the example graphs of Fig. 2. The measurements were designed so that the heating rates at the various amplitudes stayed about constant, i.e. $A_{T_s}\omega$, the maximum heating and cooling rate, $dT_s/dt$, is constant at 3.8 K/min. A plot of thus obtained glass transition behavior is shown in Fig. 4. The glass transition temperature is shifted to lower temperature with decreasing frequency $\omega$ (increasing $p$ and $A_{T_s}$).

The results of kind 2) are illustrated in Fig. 5. The chosen conditions were a linear heating and cooling rate $q = 1$ K/min, modulated with maximum heating and cooling rates of 1.18, 4.7, and 47 K/min, but at constant frequency ($p = 80$ s), corresponding to be the chosen maximum amplitudes $A_T = 0.25$, 1.0, and 10 K, respectively. The resulting glass transitions are 368.2, 368.5, and 367.5 K, respectively, i.e. they are within experimental accuracy unchanged. The lowest modulated temperature amplitudes (heating and cooling rates) give the sharpest glass transition. The differences in glass transition temperature between heating and cooling are between 0.2 and 0.35 K, also small enough to be within experimental error.

The final data series [kind 3] shows the hysteresis behavior, as illustrated in the example of Fig. 3. The samples were held for various times at temperatures 0 to 18 K below the glass transition temperature to anneal. The reversible heat capacity is shown in Fig. 6, revealing a small spread of the heat capacity in the low-temperature side of the glass transition region, but overall, only a change in $T_g$ of about 1 K. The sample with the lowest annealing temperature shows the sharpest glass transition. The irreversible (hysteresis) effect on the heat capacity in the glass transition region is collected in Fig. 7, with the lowest annealing temperature showing the highest peak temperature. As expected, the end of hysteresis is reached at the same temperature for all measurements.

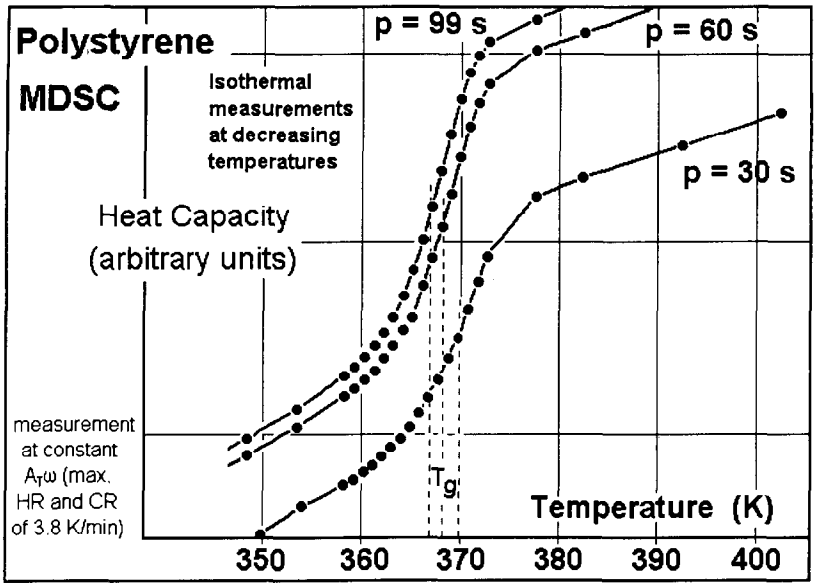


Fig. 4. Change of the glass transition with frequency at constant maximum (3.8 K/min) heating and cooling rates. Experiments of kind 1). The curves are shifted vertically by arbitrary amounts.

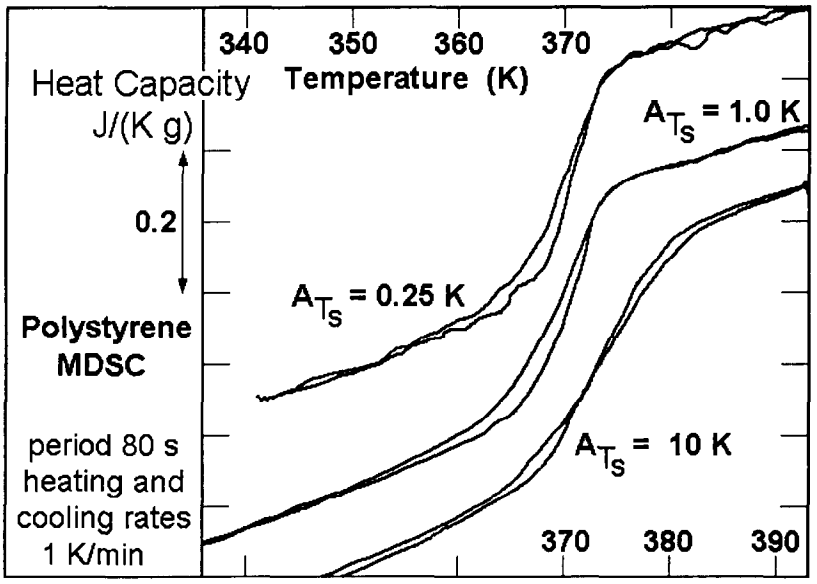


Fig. 5. Heat capacity at constant frequency ($p = 80$ s) and underlying heating rate ($q = 1$ K/min), but different modulation amplitudes. The maximum heating and cooling rates due to modulation are 1.18, 4.71, and 47.12 K/min (from top to bottom).

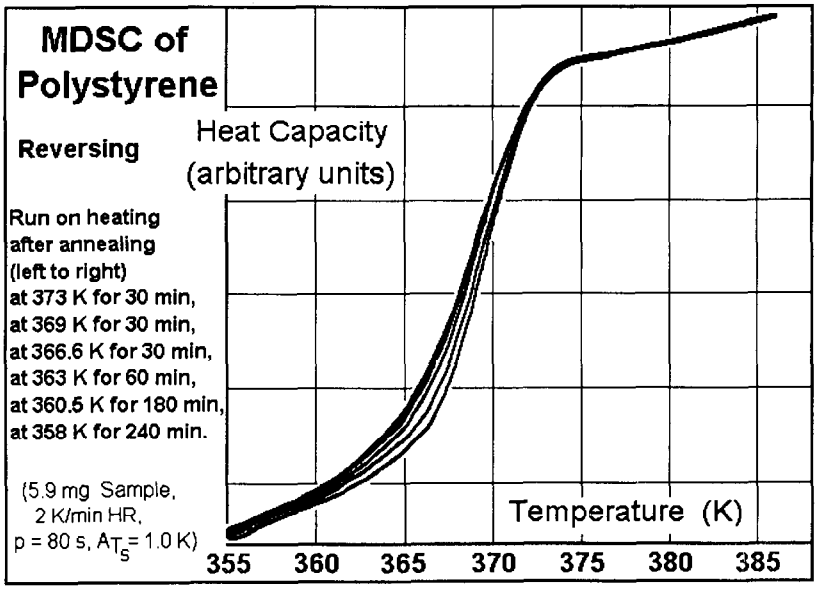


Fig. 6. Reversing heat capacity on increasing annealing (left to right), analyzed at constant underlying heating rate (2 K/min), frequency ($p = 80$ s), and amplitude ($A_{T_s} = 1.0$ K).

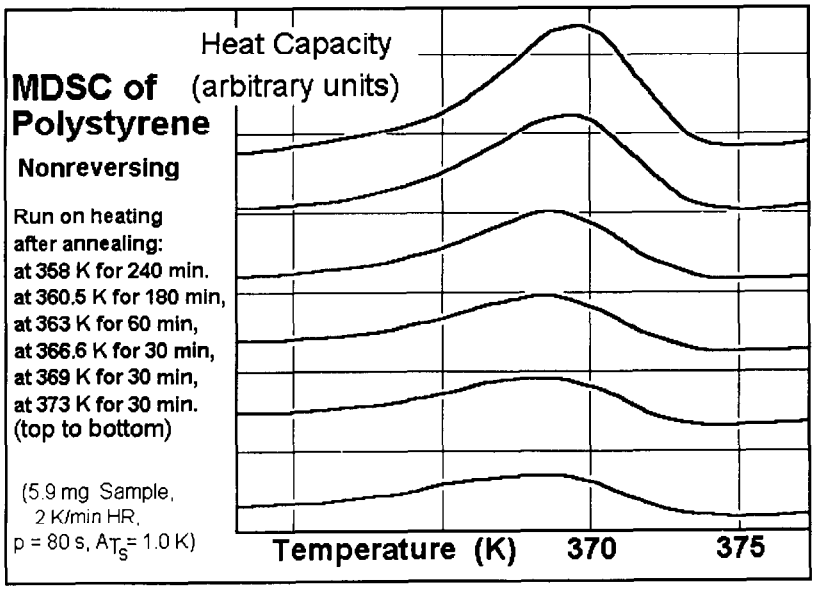


Fig. 7. Nonreversing heat capacity for the measurements indicated in Fig. 6. For an example of the separation of the nonreversing heat capacity and the total heat capacity see Fig. 3.

## 4. Interpretation of the MDSC in the glass transition region

A qualitative analysis of the superposition of the reversible and irreversible processes in the glass transition region is schematically illustrated in Fig. 8. Somewhat below the glass transition temperature, $T_g$, the heat capacity follows any change of the temperature practically instantaneously. Molecular dynamics simulations have shown that for solid polymers the time involved to reach a steady state temperature is in the picosecond range ($10^{-12}$ s) [25]. One can, thus, write the solid heat capacity simply as the vibrational heat capacity $C_{p_o}$:

$$C_p(\text{solid}) = C_{p_o} \tag{8}$$

The vibrational heat capacity $C_{p_o}$ is available through the Advanced Thermal Analysis System, ATHAS [26]. Other contributions to $C_p$(solid) are usually negligible. The parallel thin lines in Fig. 8 represent the enthalpies $H\,(=\int C_p\,dT)$ of various glasses that were cooled at different rates (higher cooling rates for larger values of $H$). Once in the glassy state, all heat capacities are closely similar (but not the enthalpies).

In the liquid state, longer times are necessary to reach thermal equilibrium because of the need of the molecules to undergo larger, cooperative, structural changes. A simple model for the representation of these motions has been given by Eyring and Frenkel [27] in terms of a hole theory, i.e. the larger expansivity of liquids and the slower response to external forces is said to be due to changes in an equilibrium of holes (of equal sizes and a temperature-dependent number). The equilibrium number of holes is $N_h^*$, each contributing an energy $\varepsilon_h$ to the enthalpy. The hole contribution to the heat

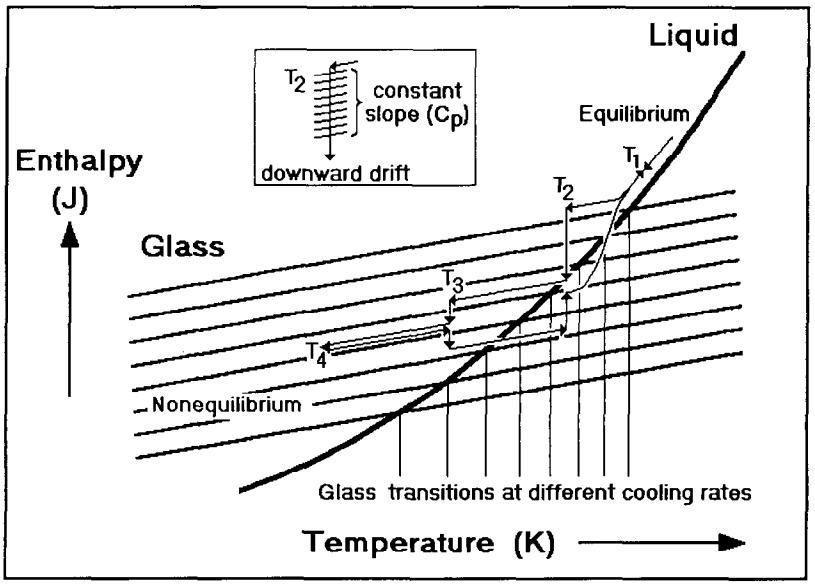


Fig. 8. Schematic of the enthalpy of glasses of different thermal history. For comparison, with Fig. 4, $T_1$ could be about 375 K, $T_2$ about 365 K.

capacity is then given by the change in number of holes with temperature under equilibrium conditions:

$$C_p(\text{liquid}) = C_{p_0} + \varepsilon_h\left(\frac{dN_h^*}{dT}\right) \tag{9}$$

Creation, motion, and destructions of holes are, however, cooperative kinetic processes and may be slow. This leads to deviations from Eq. (9) if the measurement is carried out faster than the kinetics allows. Applied to the glass transition, one can write a simple, first-order kinetics expression [28] that has been extended to describe the time-dependent, apparent heat capacity in the glass-transition region [18]:

$$\left(\frac{dN_h}{dt}\right) = \frac{1}{\tau}(N_h^* - N) \tag{10}$$

with $N$ representing the instantaneous number of holes, and $N_h^*$, the equilibrium number of holes; $\tau$ is the relaxation time for the formation of holes. Both $N_h^*$ and $\tau$ are available through the hole theory [27].

Some five to ten kelvins above $T_g$, most one-phase and one-component systems show no kinetic effects for DSC heating or cooling rates typically used (1–20 K/min). The heat capacity is then equal to the slope of the heavy curve in Fig. 8. On going through $T_g$, the glassy state is reached at different temperatures for different cooling rates. Each cooling rate corresponds to freezing-in a different number of holes, giving rise to the multitude of glasses with different enthalpies indicated in Fig. 8. Using MDSC, the slope of the enthalpy of these glassy states can be measured. As indicated in the figure all slopes are practically the same, irrespective of the actual enthalpy level. In the temperature range were modulation frequency and relaxation times are comparable, Eq. (10) must be considered.

The next more detailed analysis involves step-wise cooling and heating with long-time quasi-isothermal, modulated measurements between $T_1$ and $T_4$. At $T_1$ the heat capacity is represented by Eq. (9), the modulation is slow enough to be followed by the kinetics. Cooling quickly to $T_2$ yields initially a glass, represented by the upper thin enthalpy line. At this temperature the modulation frequency is already too fast to measure anything but the heat capacity of the glass given by Eq. (8). Since the measurement is carried out over many modulation cycles, the enthalpy relaxes slowly in an irrversible process to the lower levels of enthalpy (as indicated by the vertical arrow). These enthalpy changes are little affected by the small temperature changes due to modulation, and thus not measured by MDSC. The center insert illustrates this downward drift that can be computed with use of Eq. (10). Even if ultimately the equilibrium liquid were reached, as suggested in the figure, the measured heat capacity would still be that of the solid, since the hole equlibrium does not change significantly during the modulation period. Continuing to $T_3$, the enthalpy relaxation is less, but again unrecorded by MDSC. At $T_4$, finally, a metastable glass has been reached. On reheating, the relaxations at $T_3$ and $T_2$ would, again, not be recorded (note the different directions of the relaxation for $T_1$ and $T_2$). During the jump to $T_1$ the relaxation time is sufficiently short that the hole contribution can be measured and $C_p$ is again repre-

sented by Eq. (9). On the cooling, as well as on the heating run the heat capacity between $T_1$ and $T_2$ is intermediate between Eqs. (8) and (9), giving a glass transition temperature at half-vitrification [29] that is governed only by the time scale of modulation. In this way MDSC is able to establish a precise (modulation frequency dependent) glass transition temperature on cooling as well as on heating. Normal DSC is unable to do the latter, because of the simultaneous recording of heat capacity and enthalpy relaxation. Special methods are necessary to extract the glass transition from a DSC trace measured on heating and showing enthalpy relaxation. Even if these methods are followed, one can only assess the glass transition corresponding to the prior cooling rate (thermal history) [7]. Continuous heating and cooling experiments give a continuous recording, blurred somewhat over the temperature range of modulation.

## 5. Discussion

Figs. 3–7 indicate that, indeed, the irreversible hysteresis effect and the frequency-dependent reversing heat capacity of polystyrene can be separated, and the approximate analysis of Fig. 8 is qualitatively useful. This separation of the intrinsic glass transition and the hysteresis effect should permit an independent discussion of the glass transition of the glass measured on heating or on cooling and the thermal history (or ageing). One can also suggest that the rather difficult analysis of mechanical history may be quantitatively separated from the underlying glass transition.

More quantitative information on the time and temperature dependence of the glass transition is available from Fig. 4. Increasing the modulation frequency by a factor of three at constant maximum heating rate increases the glass transition temperature by about 2 K. The same shift ($\Delta$) is shown between storage modulus curves in Fig. 9. These literature data were measured on similar polystyrene for the elastic modulus with dynamic mechanical analysis (DMA) at constant temperatures with similar frequencies [30]. Although the range of frequencies in the MDSC experiments is small, one expects a similar apparent activation energy as found (with additional frequencies) in the DMA experiment (812 kJ /mol) [30]. This, in turn, agrees with the commonly accepted values in the literature [31]. Another question concerns the choice of the glass transition temperature. From the MDSC data it is easy to find the "temperature of half-vitrification" [29] at about 368 K. Since heat capacity is an extensive quantity, this definition has a clear operational meaning. Young's modulus, however, is an intensive quantity, and an operational meaning can only be attached to the extensive retracting force in linear, not logarithmic units. Finding the decrease in this force by 50% (after correction for the change of the glassy behavior with temperature) leads to the beginning of the decrease in modulus, and agrees, again reasonably well with the DSC data, as indicated in Fig. 9. The peak of the loss tangent is, in contrast, almost 15 $K$ higher than the inital decrease of the storage modulus [30]. The easily recognizable loss peak, that has been claimed to make DMA 1000 times more sensitive for identifying the glass transition [32], is thus only indirectly related to the glass transition temperature.

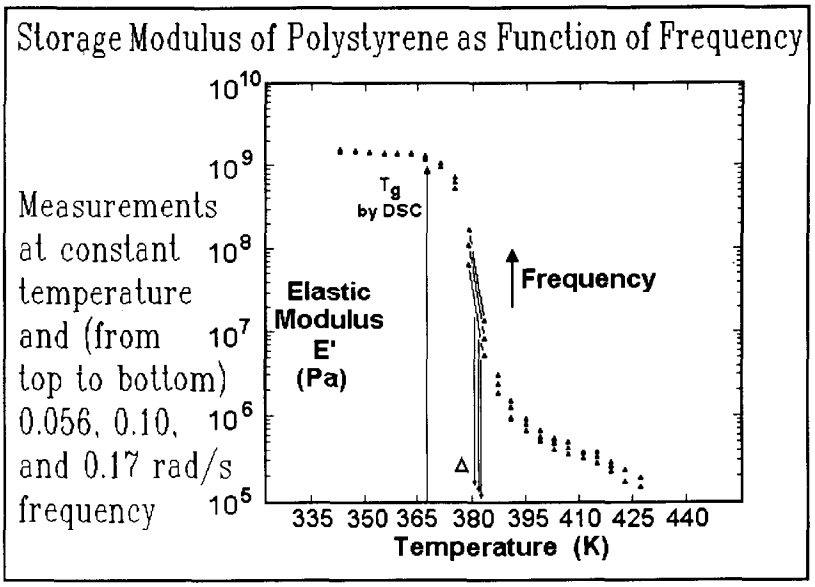


Fig. 9. Logarithm of the elastic storage modulus of polystyrene at constant temperatures, approximately matching the frequencies of Fig. 4. Drawn after Ref. [30].

The initial change in storage modulus is naturally much more difficult to establish. To make a quantitative comparison, it would be necessary to use all methods on the same sample and go beyond the usual empirical descriptions. The MDSC seems to offer this opportunity.

The measurement at constant heating and cooling rates (second kind of experiment) shows agreement between heating and cooling data for the reversing signal within the experimental precision. A broadening of the glass transition in Fig. 5 becomes obvious when the modulation amplitude exceeds the inherent breadth of the glass transition region (about 10–15 K, as seen from Fig. 4). Increasing the heating and cooling rates increases the glass transition, as is known from the earlier experiments [24]. The earlier DSC data agree, again, approximately with recent comparable data by DMA [31].

The analysis of the third kind of experiment displayed in Figs. 3, 6, and 7 allows the study of the ageing of a sample without being bound to the initial cooling condition for the evaluation of the enthalpy relaxation [7] that is often cumbersome to establish [33]. Although the reversing part of the heat capacity after the annealing is approximately constant, it is not exactly so. The samples of higher ageing (larger hysteresis peak in Fig. 7) show a higher and narrower glass transition temperature region (however, with the same upper temperature limit). It should be possible to evaluate these changes quantitatively in an effort to establish a more than empirical description of the hysteresis phenomenon. As in the earlier work in which the hole theory was used [24], one must conclude that the change in the glass transition range in Fig. 6 is due to an increasingly cooperative behavior of the more annealed samples.

## 6. Conclusions

The experiments displayed in this report indicate that MDSC is a new tool for the quantitative analysis of the glass transition temperature. The advantage of the existing operational definition of the glass transition using heat capacity should help in developing a more fundamental interpretation of the data and resolve the remaining differences beween thermal and mechanical data. The MDSC method permits the measurement of the glass transition temperature on heating, unimpeded by thermal history. The data are dependent on the modulation frequency, just as mechanical and dielectric data are [14]. A simple interpretation of the data is possible using an enthalpy discussion in the frame of the hole theory kinetics (Fig. 8). As in the earlier attempt of a discussion of the kinetics, full correspondence cannot be achieved until a better understanding of the cooperative behavior of the large-amplitude motion in the glass transition region is developed. Modulated DSC may be able to help in the generation of data for this effort, as shown in Fig. 6.

## Acknowledgements

The authors greatfully acknowledge extensive discussions with Drs. M. Reading, ICI Paints; B.S. Crowe, TA Instruments; and all attendees at the Third Lähnwitz seminar, 1994. This work was supported by the Division of Materials Research, National Science Foundation, Polymers Program, Grant # DMR 90-00520 and the Division of Materials Sciences, Office of Basic Energy Science, U.S. Department of Energy, under Contract DE-AC05-84OR21400 with Lockheed Martin Energy Systems, Inc.

## References

[1] M. Reading, D. Elliot and V.L. Hil, J. Thermal Anal., 40 (1993) 949.
[2] P.S. Gill, S.R. Sauerbrunn and M. Reading, J. Thermal Anal., 40 (1993) 931.
[3] M. Reading, Trends in Polymer Sci., 8 (1993) 248.
[4] M. Reading, B. Hahn and B.S. Crowe, US Patent 5,224,775 (July 6, 1993).
[5] Y. Jin, A. Boller and B. Wunderlich, in Proc. 22nd NATAS Conf., Denver, Co. September 19–22, K.R. Williams, ed., pgs. 59–64 (1993); see als, A. Boller, Y. Jin and B. Wunderlich, J. Thermal Analysis, 42, (1994) 307.
[6] B. Wunderlich, Y. Jin and A. Boller, Thermochim. Acta, 238 (1994) 277.
[7] B. Wunderlich, Thermal Analysis, Academic Press, Boston, 1990.
[8] W. Hemminger and G. Höhne, Calorimetry, Verlag Chemie, Weinheim, 1984.
[9] B. Wunderlich and J. Grebowicz, Thermotropic Mesophases and Mesophase Transitions of Linear, Flexible Macromolecules Adv. Polymer Sci, 60/61, (1984) 1.
[10] G.W. Grey, Molecular Structure and the Properties of Liquid Crystals. Academic Press, New York, 1962.
[11] N. Sherwood, ed., The Plastically Crystalline State. Wiley, Chichester, 1979.
[12] B. Wunderlich, M. Möller, J. Grebowicz and H. Baur, Conformational Motion and Disorder in Low and High Molecular Mass Crystals. Springer Verlag, Berlin, 1988, (Adv. Polymer Sci., Volume 87).
[13] G. Tammann, Der Glaszustand Leopold Voss, Leipzig, 1933.

[14] R.G. Seyler, editor, Assignment of the Glass Transition, ASTM Symposium, March 4–5, 1993, Atlanta, CA. STP 1249, Am. Soc. Testing of Materials, Philadelphia, 1994.
[15] B. Wunderlich, Colloid and Polymer Sci., 96 (1994) 22.
[16] D. Vorlaender, Trans. Farad. Soc., 29 (1933) 207.
[17] K. Tsuji, M. Sorai and S. Seki, Bull. Chem. Soc., Japan, 44 (1971) 1452.
[18] M. Sorai and S. Seki, Mol. Cryst. Liq. Cryst. 23 (1973) 299.
[19] M. Sorai, H. Suga, S.H. Yoshioka and S. Seki Mol. Cryst. Liq. Cryst. 59 (1980) 33; 73 (1981) 47; 84 (1982) 39.
[20] K. Adachi, H. Suga and S. Seki, Bull. Chem. Soc., Japan, 41 (1968) 1073; 43 (1970) 1916; 44 (1971) 78; O. Haida, H. Suga and S. Seki, Chem. Letters, (1973) 79.
[21] D.A. Ditmars, S. Ishihara, S.S. Chang, G. Bernstein and E.D. West, J. S. Res. Natl. Bur. Stand., 87 (1982) 159.
[22] Y. Jin, A. Xenopoulos, J. Cheng, W. Chen, B. Wunderlich, M. Diak, C. Jin, R.L. Hettich, R.N. Compton and G. Guichon, Mol. Cryst. Liq. Cryst., 257 (1974) 235.
[23] U. Gaur and B. Wunderlich, J. Phys. Chem. Ref. Data 11 (1982) 313.
[24] B. Wunderlich, D.M. Bodily and M.H. Kaplan, J. Appl. Phys., 35 (1964) 95.
[25] B.G. Sumpter, D.W. Noid and B. Wunderlich, Atomistic Dynamics of Macromolecular Crystals. Springer Verlag, Beling, Adv. Polymer Sci., 116, 27 (1994). Volume on "Atomistic Modelling of Physical Properties of Polymers."
[26] Contact the authors for the latest summary, see also Ref. [7], or B. Wunderlich, The Advanced Thermal Analysis System, ATHAS, Shin Netsu Sokuteino Shinpo, 1 (1990) 71. See also: Pure and Appl. Chem., 67 (1995) 1919.
[27] H. Eyring, Chem. Phys., 4 (1936) 238; J. Frenkel, Kinetic Theory of Liquids. Clarendon Press, Oxford, England, 1946.
[28] N. Hirai and H. Eyring, J. Appl. Phys., 29 (1958) 810; J. Polymer Sci., 37 (1959) 651.
[29] B. Wunderlich, The Nature of the Glass Transition and its Determination by thermal Analysis, Ref. 14 page 75.
[30] E.L. Rodriguez, The Glass Transition Temperature of Glassy Polymers Using Dynamic Mechanical Analysis., Ref. 14, page 255.
[31] See, for example, J.D. Ferry, Viscoelastic Properties of Polymers, third ed., J. Wiley and Sons., New York, NY, 1980; or N.G. McCrum, B.E. Read, G. Williams, Anelastic and Dielectric Effects in Polymeric Solids, Dover Publ., New York, NY, 1991.
[32] J. Foreman, S.R. Sauerbrunn and C.L. Marcozzi, Proc. 22nd NATAS Conference, Denver, Sept. 19–23, Ed. K.R. Williams, 1993.
[33] R.J. Roe, J.J. Curro and S.K. Lo, ACS Preprints, 17(2) (1977) 167.